TEKNIK

Tersedia online di: http://ejournal.undip.ac.id/index.php/teknik

TEKNIK, 44 (2), 2023, 123-129

Mg-0.5Ca-4Zn-xCaCO3 (x=8, 10) Alloy Foams with Closed-Pore Structure Synthesized by Powder Metallurgy Process for Implant Applications

Aprilia Erryani*, Franciska Pramuji Lestari, Joko Triwardono, Bunga Rani Elvira, Bintoro Siswayanti, Albertus Deny Heri Setyawan

Research Center for Metallurgy, National Research and Innovation Agency (BRIN), KST B.J. Habibie, Jl. Raya Puspiptek Serpong Gd. 720, Tangerang Selatan, Banten 15314, Indonesia

Abstract

This work aims to synthesize Mg-0.5Ca-4Zn alloy foams using a CaCO3 foaming agent and a powder metallurgy (PM) process. Mg-0.5Ca-4Zn-xCaCO3 (x=8, 10 wt.%) alloy precursors were prepared by mixing Mg, Ca, and Zn metal powders with CaCO3 granules, compacting, and then sintering at various temperatures (i.e., 650, 675, and 700 °C) for 5 hours in an argon atmosphere. The pore morphology was observed by scanning electron microscopy (SEM), and the phase formation was analyzed using X-ray diffractometry (XRD). The density and porosity were evaluated using an Archimedes test (ASTM B311-93). The compressive strength was examined using a universal testing machine (UTM) with a constant crosshead speed of 1.3 mm/min (ASTM D695-02). SEM observation reveals the formation of pores with a closed-cell type structure in all alloy compositions. Increasing either the CaCO3 content or sintering temperature results in an increase in porosity and pore sizes but a decrease in compressive strength. The maximum porosity of 43.208% was obtained in the alloy foam with 10 wt.% CaCO3 sintered at 700 °C; the foam exhibits a compressive strength of 52.9 MPa, close to cancellous bone.

Keywords: *alloy foam; CaCO3 foaming agent; Mg-Zn-Ca alloys; closed-pore structure*

1. Introduction

Magnesium is a potential candidate as a material for biodegradable orthopedic implants since its mechanical properties are very similar to those of human bone, and Mg itself is one of the essential elements in the human body (Salleh *et al*., 2016; Lietaert *et al*., 2013). The density (ρ) and elastic modulus (E) of Mg are 1.738 g/cm^3 and 45 GPa, respectively, which are closely comparable to those of human bone (i.e., ρ_{bone} = 1.8–2.1 g/cm^3 and E_{bone} = 40-57 GPa) (Peron *et al.*, 2017). However, magnesium has poor forming ability, limited ductility at room temperature, and low corrosion resistance. Therefore, appropriate alloying elements are critical to improve the properties (Doležal *et al*., 2016; Sahinoja, 2013; Ding *et al*., 2014). Zn is one of the most potential alloying elements for improving the mechanical properties and corrosion resistance of Mg alloys. However, the Zn content as the alloying element should not exceed 5 wt.%; otherwise, the corrosion properties deteriorate (Cai *et al*., 2012). Similarly, Ca is a crucial element in human bones and contributes to improving the corrosion resistance and mechanical properties of Mg alloys (Lu, 2014). Ca may enhance oxidation resistance by forming protective oxide layers and increase hardness and creep resistance by forming a Mg_2Ca intermetallic compound (Hussein & Northwood, 2014; Harandi *et al*., 2013). With this regard, Mg-Ca-Zn alloys have been thoroughly investigated as one of the materials potential for biomedical applications (Hofstetter *et al*., 2014; Lu, 2014; Doležal *et al.*, 2016; Tu *et al*., 2019; Dargusch *et al.*, 2022).

A metal or alloy foam is attractive for implant applications because its porous structure resembles human bone, and the foaming process is controllable to produce a porous material with excellent biocompatibility (Osorio-Hernández et al., 2014). Porous implants are classified into two types: closed pores and open pores. On the outside of the bone are closed pores like dense bone (cortical bone). The open pores resemble the inner bone (cancellous bone) whose pores are connected (Osorio-Hernández et al., 2014). The foaming process can be performed by utilizing the decomposition reaction of a foaming agent in molten metal or alloy. TiH_2 has been used widely as a foaming

*) Corresponding author.
E-mail: aprilia.erryani@gmail.com

doi: 10.14710/teknik.v44i2.49587

agent to synthesize Al alloy foams (Gonzales *et al*., 2013; Lestari *et al*., 2020). However, the TiH_2 releases H_2 gas, which is hazardous and flammable, during the decomposition; hence, it is unsuitable for foam Mg alloys with high activity at high temperatures. On the other hand, $CaCO_3$ is an attractive foaming agent because it is inexpensive and less hazardous. At high temperatures, $CaCO_3$ decomposes by releasing CO gas, which can generate pores in Mg alloys (Kennedy, 2012; Erryani *et al*., 2015).

A foaming process can be performed by mixing and stirring foaming agents directly in a metal/alloy melt. This method, however, is costly since it requires quite a high temperature (i.e., above the melting point of the metal/alloy) and relatively complex equipment to accommodate the foaming process. In addition, the homogeneity and alloy composition are also challenging to control. A more simple and budget-friendly powder metallurgy (PM) process can be used as an alternative to synthesizing Mg alloy foams. In the PM process, the foaming agent ($CaCO_3$) is distributed properly within a Mg alloy precursor and then heated to release gas during the decomposition at an elevated temperature.

Works on the Mg-Ca-Zn alloy foams are still limitedly reported. Previous works investigated Mg-Ca-Zn porous alloys with different alloy compositions and/or foaming agents (Erryani *et al.*, 2015; Lestari *et al*., 2020). However, the alloy composition and process are still necessary to optimize. Ca content needs to be suppressed since it is difficult to handle and easily oxidized, especially in the form of fine particles. Zn should also be limited because an excessive Zn content degrades the corrosion properties.

This work, therefore, aims to synthesize Mg-Ca-Zn alloy foams with closed-pore structure by employing a simple PM technique. A newly developed Mg-0.5Ca-4Zn alloy and inexpensive $CaCO_3$ as the foaming agent are used for this purpose. The effects of $CaCO_3$ content and sintering temperature on the pore characteristics and mechanical properties are investigated and discussed.

2. Materials and Method

Materials used in this work were the commercial powders of Mg (Merck, 98.5 % purity, particle size (D) = 0,06-0,3 μm), Ca granules (Merck, 98 % purity), Zn (Merck, 99 % purity, D < 45 μm), and with $CaCO_3$ fine granules (Merck, 98.96% purity, D < 30 μm) as the foaming agent. Those materials were mixed to compose alloys with a nominal composition of Mg-0.5Ca-4Zn-x$CaCO_3$ (x=8, 10 wt.%).

The Mg, Ca, Zn, and $CaCO_3$ powders were initially blended using a shaker mill at room temperature for 30 min. Cylindrical green compacts (10 mm in diameter and 10 mm in thickness) were then prepared by uniaxially compacting the powder mixtures at room temperature. The pressure was applied in two steps: 100 MPa for 2 minutes and 200 MPa for 3 minutes. The green compacts (precursors) were subsequentially sintered in a tubular furnace with an argon atmosphere at 650, 675, and 700 ºC for 5 hours (Erryani *et al.*, 2015; Lestari *et al*., 2020). The sintering temperatures (T_{sinter}) were determined based on the differential thermal/thermogravimetric analyses (DTA/TGA) performed for the $CaCO_3$ powder and Mg-Ca-Zn-$CaCO_3$ (hereon, it is denoted as MgAlloy-$CaCO_3$) powder mixture using LINSEIS STA (simultaneous thermal analyzer) Platinum Series.

The microstructure and pore morphology of the sintered samples were observed by a JEOL JSM-6390A scanning electron microscope (SEM) equipped with an energy dispersive spectrometer (EDS). An X-ray diffractometer (XRD) with Cu-Kα radiation was used to analyze the phase formation in the samples.

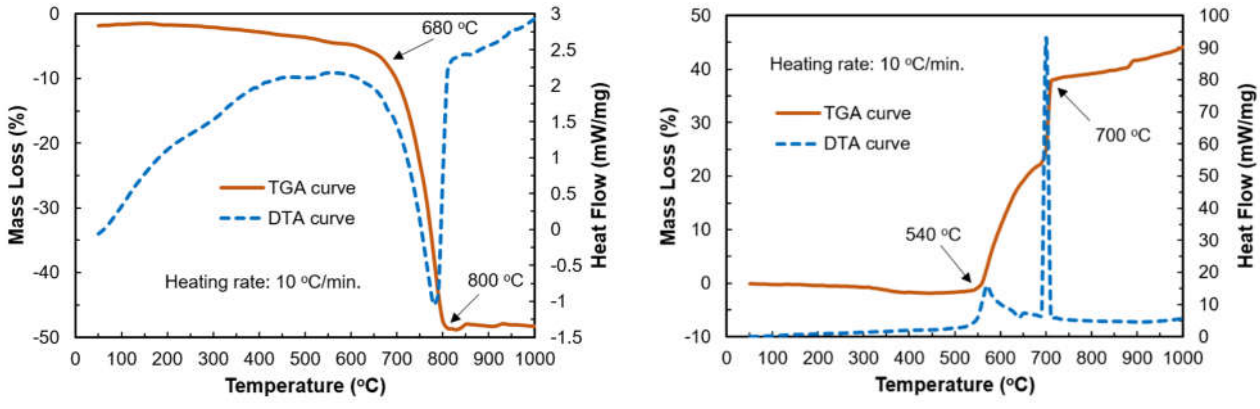

Figure 1. DTA/TGA curves of the (a) $CaCO_3$ powder and (b) MgAlloy-$CaCO_3$ precursor.

doi: 10.14710/teknik.v44i2.49587

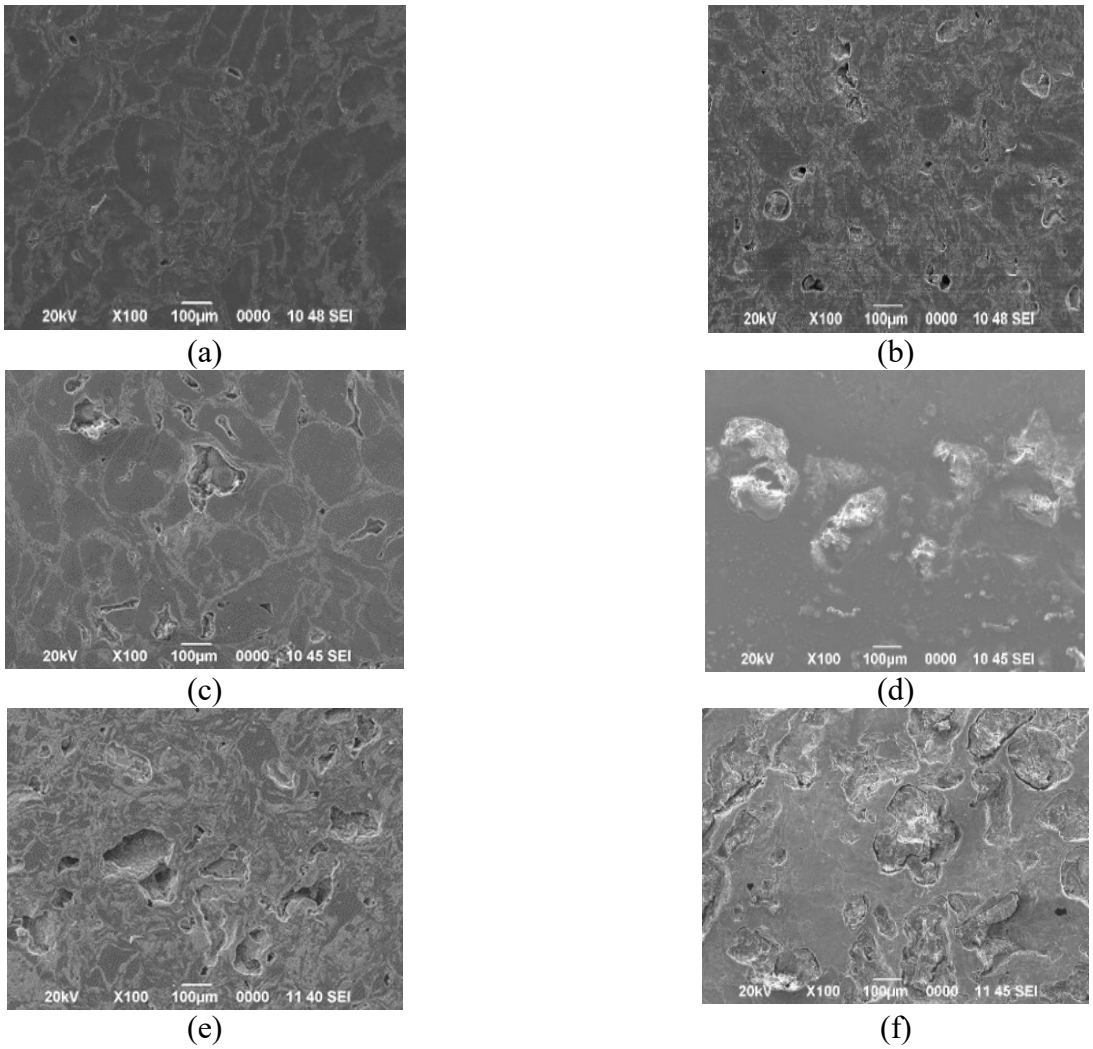

Figure 2. SEM micrographs of Mg-0.5Ca-4Zn-x$CaCO_3$ of various sintering temperatures (T_{sinter}, °C) and CaCO3 contents (x, wt.%): (a) T=650/x=8, (b) T=650/x=10, (c) T=675/x=8, (d) T=675/x=10, (e) T=700/x=8, and (f) T=700/x=10.

An Archimedes test evaluated the sample's density and porosity according to ASTM B311-93. The sample density was calculated using Equation (1).

$$\rho_b = \frac{m_1}{m_3 - m_2} \times \rho_{air} \quad (1)$$

where ρ_b = the theoretical density (gr/cm^3), m_1 = sample dry weight (gram), m_2 = sample weight in water (gram), m_3 = wet sample weight (gram), and ρ_{water} = water density (gr/cm^3).

The porosity was then calculated using Equation (2).

$$\mu = 1 \quad \frac{\rho_t}{\rho_b} \times 100\% \quad (2)$$

where μ = porosity, ρ_b = wet density (gr / cm^3), ρ_t = dry density (gr / cm^3).

The compressive test was carried out at room temperature by using a universal testing machine (UTM) Shimadzu AGS-10 KN with a constant crosshead speed of 1.3 mm/min. (ASTM D695-02).

3. Results and Discussion

3.1 Thermal Analysis

Fig. 1(a) and (b) show DTA/TGA curves of $CaCO_3$ powder and MgAlloy-$CaCO_3$ powder mixture, respectively. An exothermic reaction accompanied by a weight change is seen clearly, starting and ending at approximately 680 ºC and 800 ºC, respectively, for the $CaCO_3$ powder (Fig. 1(a)). This reaction corresponds to the decomposition of $CaCO_3$ into CO_2 and CaO (Fedunik-Hofman *et al.,* 2019).

doi: 10.14710/teknik.v44i2.49587

Table 1. Relative element-composition identified by EDS in the Mg-0.5Ca-4Zn-x$CaCO_3$ (x=8, 10 wt.%) alloys sintered at various temperatures

Element	T_{sinter}=650 ºC		T_{sinter}=675 ºC		T_{sinter}=700 ºC	
	x=8	x=10	x=8	x=10	x=8	x=10
Mg	71.93	49.99	10.18	5.35	41.56	10.65
Ca	5.88	6.08	5.36	1.38	4.02	0.65
Zn	8.99	18.34	5.54	2.83	5.70	0.75
C	3.18	10.75	39.73	46.54	26.64	46.14
O	10.01	14.84	39.19	43.90	22.08	41.81

In the MgAlloy-$CaCO_3$ powder mixture, decomposition occurs at a lower temperature range than in the $CaCO_3$ (Fig. 1(b)). The decomposition of MgAlloy-$CaCO_3$ starts at 540 ºC and ends at 710 ºC.

The foaming process of MgAlloy-$CaCO_3$ follows the reaction 3 (Lu *et al*., 2013).

$$Mg(s)+CaCO_3(s) \rightarrow MgO(s) + CaO(s) + CO\uparrow \quad (3)$$

Based on the DTA/TGA analysis, the sintering for MgAlloy-CaCO3 compacted samples was carried out at 650, 675, and 700 ºC, which are within the decomposition temperature range.

3.2 Pore Structure and Morphology

Figure 2 shows SEM micrographs of the sintered Mg-0.5Zn-4Ca-x$CaCO_3$ alloys. The sample microstructure consists of a primary α-Mg matrix with a secondary phase distributed along the grain boundary. The samples sintered at 650 ºC exhibit pores at the grain boundary, particularly in the sample with 10 wt.% $CaCO_3$ (Figure 2(b)); however, the pores are hardly observed in the sample with 8 wt.% foaming agent (Fig. 2(a)). The pore characteristic indicates a typical closed-pore structure with nearly equiaxed morphology, particularly in the x=10 sample. Sintering at higher temperatures (i.e., 675 ºC and 700 ºC), however, increases pore size and changes in pore morphology. Moreover, the pore morphology becomes irregular and distorted from an equiaxed shape. At T_{sinter} = 700 ºC, elongated pore cells and some buckled cell walls are observed in the x=8 sample (Figure 2(e)). Broken cell walls and non-equiaxed cells are even revealed in the x=10 one (Figure 2(f)), indicating that some pore-cells expanded and merged with their neighbors.

Pores are formed by the decomposition of foaming agents during the sintering process. Varying sintering temperatures and the content of foaming agents results in different types of pore morphology. (Yusop et al., 2012). In this regard, increasing the $CaCO_3$ content or sintering temperature causes the intensification of $CaCO_3$ decomposition and, hence, results in pore expansion and coalescence, as shown the Figures 2(e) and (f). The pore structure formed in the present alloy foams is a closed-pore type since a complete interconnection among the pores is hardly observed. The results indicate that the powder metallurgy process (i.e., powder mixing, compacting, and sintering) is possible for the pore formation in the alloy samples.

3.3 Structure and Phase Identification

Table 1 shows the relative composition among the elements of the sintered Mg-0.5Ca-4Zn-x$CaCO_3$ alloys analyzed by EDS. It is seen that Mg, Ca, and Zn are dominant, while the C and O contents are relatively low in the alloys sintered at 650 ºC compared to those of higher temperatures (675 ºC and 700 ºC). This indicates that the decomposition of $CaCO_3$ has not or only partially occurred at T_{sinter} =650 ºC.

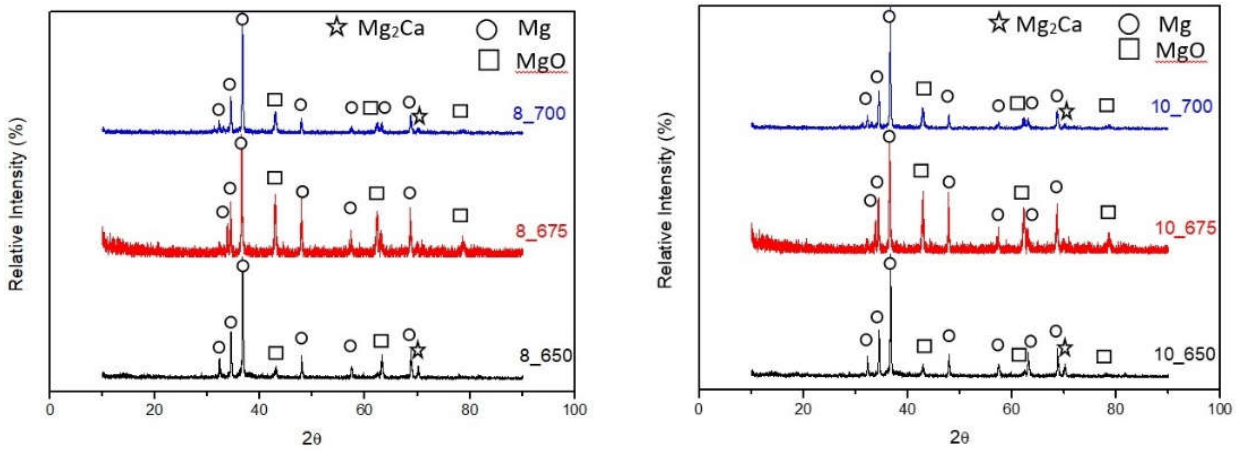

Figure 3. XRD patterns of Mg-0.5Ca-4Zn-x$CaCO_3$ alloy foams produced from various sintering temperatures for (a) x=8 and (b) x=10 (wt.%).

doi: 10.14710/teknik.v44i2.49587

Table 2. Density, porosity, and compressive strength of Mg-0.5Ca-4Zn-x$CaCO_3$ (x=8, 10 wt.%) alloy foams.

x (wt.%) - T_{sinter} (°C)	Density (gr/cc)	Porosity (%)	Compressive Strength (MPa)
8 - 650	1.493	21.097	111.2
10 - 650	1.489	23.729	105.8
8 - 675	1.458	25.313	88.0
10 - 675	1.437	27.484	86.7
8 - 700	1.301	33.336	58.2
10 - 700	1.142	43.208	52.9

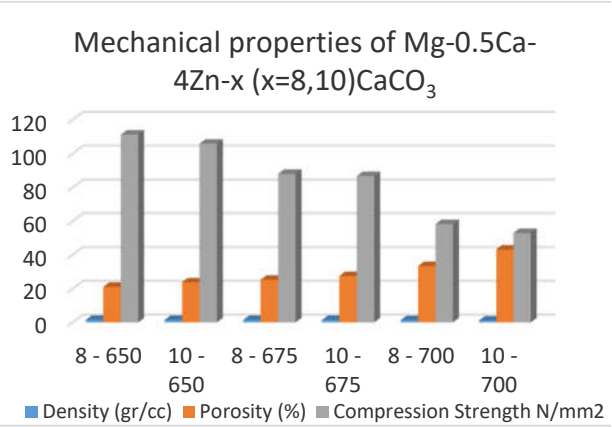

Figure 4. Mechanical properties of Mg-0.5Ca-4Zn-x $CaCO_3$ (x=8, 10 wt.%) alloy foams produced from various sintering temperatures.

The dominant content of Mg, Ca, and Zn in these alloys also suggests the formation of the Mg-Ca and/or Mg-Zn intermetallic phase(s). In fact, some Mg-Ca and Mg-Zn intermetallic compounds were reported to form in the grain boundary of Mg-Zn-Ca alloys with high Zn content (Annur *et al*., 2016). On the other hand, C and O contents are much higher than the other elements in the alloys sintered at 675 ºC and 700 ºC, indicating the intensification of $CaCO_3$ decomposition. This result agrees well with the pore structure evolution detected by SEM, shown in Figure 2.

The XRD patterns of the alloys after the sintering show the formation of MgO and Mg2Ca phases in addition to the primary Mg as the dominant component (Figure 3). MgO phase formed due to the decomposition of MgAlloy-$CaCO_3$, as shown in the reaction (3). Meanwhile, the formation of Mg_2Ca phase occurred because the Ca addition reached the critical amount for this phase formation in a Mg-Ca-Zn alloy. The Mg_2Ca phase formed in the Mg-Ca alloys with Ca > 0.5 wt.% (Rad *et al.,* 2012; Zeng *et al*., 2015). The formation of Mg2Ca phase takes place mainly at the grain boundary (Schaublin *et al.,* 2022). However, there was no Mg2Ca phase at 675 ºC. This is because $CaCO_3$ was not completely dissolved during the sintering process. Thus, the Mg_2Ca phase does not develop.

3.4 Mechanical Properties

Table 2 and Figure 4 show the density, porosity, and compressive strength of Mg-0.5Ca-4Zn-x$CaCO_3$ alloy foams synthesized at various sintering temperatures. The sample density decreases with the increase of $CaCO_3$ content or T_{sinter}. This is certainly because of the increase in porosity in the alloy foams with a higher $CaCO_3$ content or fabricated from a higher sintering temperature due to the intensification of $CaCO_3$ decomposition.

The pore formation during a sintering process depends on the amount of foaming agent and sintering temperature. The greater amount of foaming agents, the higher possibility of pore formation. The higher the sintering temperature, the more pores may develop (Seyedraoufi & Mirdamadi, 2013). Furthermore, the higher sintering temperature, the greater the decomposition rate of CO gas within Mg-Ca-Zn alloys. Thus, increases the pore's size and numbers and leads to more homogenous pore distribution (Yang *et al.*, 2017).

From the DTA/TGA result, the decomposition temperature of $CaCO_3$ in Mg alloy is 540–710 ºC, in which the CO gas is released from the reaction of Mg alloy with $CaCO_3$ (Figure 1 and Equation 3). The formation of CO gas leads to the production of pores. The pores start to develop in the sample with 10 wt.% $CaCO_3$ sintered at 650 ºC. They expand and begin to coalesce as the content of the $CaCO_3$ foaming agent and sintering temperature increase. In the present alloys, however, the pore evolution did not lead to a full interconnection among the pores, even for the highest amount of foaming agent (x=10) and sintering temperature (700 ºC). As a result, alloy foams with a closed-cell structure were produced. The maximum porosity of 43.208 % is obtained in the alloy with 10 wt.% $CaCO_3$ sintered at 700 ºC.

The compressive strength is strongly affected by the sample's porosity. As seen in Table 2 and Figure 4, the increase in porosity leads to decreased compressive strength. The strength decreases from 111.2 MPa (in x=8, T_{sinter}=650 ºC) to 52.9 MPa (in x=10, T_{sinter}=700 ºC) inversely to the porosity, which increases from 21.097 to 43.208 %. The compressive strength of 52.9 MPa exhibited by the present alloy foam is close to that of cancellous bone, which is between 1.5 – 45 MPa (Carter & Hayes, 1977; Ginebra, 2019). The result suggests that the alloy foams are potentially applied as orthopedic implant materials. However, the optimization of fabrication parameters to produce more homogenous and

doi: 10.14710/teknik.v44i2.49587

controllable pores, as well as the examination of biocompatibility aspects, is critical.

4. Conclusion

Magnesium alloy foams have been successfully fabricated in the Mg-0.5Ca-4Zn-x$CaCO_3$ (x=8, 10 wt.%) alloys by a PM process. The foaming process is enabled by the decomposition of CaCO3 foaming agent during alloy sintering in which CO gas is released. The pore morphology showed a closed-pore type structure as observed by SEM. Close pore is identical to cortical bone where the pores are not connected to each other. The $CaCO_3$ content and T_{sinter} strongly affect the evolution of the pore structure and, hence, the alloy foams' density, porosity, and mechanical properties. The sample with x=8 wt.%/T_{sinter}=650 °C exhibits porosity and compressive strength of 21.097 % and 111.2 MPa, respectively. The properties dramatically change to 43.208 % (porosity) and 52.9 MPa (compressive strength) for the sample with x=10 wt.%/T_{sinter}=700 °C. The latter exhibits a compressive strength that is close to that of cortical bone (1.5–45 MPa). Mg-0.5Ca-4Zn-x$CaCO_3$ with T_{sinter}=700 ºC has a compressive strength closest to the cortical bone with 59.2 MPa. The results show the possibility of utilizing the PM method and $CaCO_3$ foaming agent to produce Mg-Ca-Zn alloy foams prospective for implant materials. However, further investigations concerning the optimization of fabrication parameters and the biocompatibility examination are necessary.

Acknowledgment

This research was financially supported by the Excellent Research Programme of The National Research and Innovation Agency. The authors thank the Research Group of Nonferrous Alloys, the Research Center for Metallurgy, National Research and Innovation Agency (BRIN) for supporting this research.

References

Annur, D., Lestari, F. P., Erryani, A., Amal, M. I., Sitorus, L. S., & Kartika, I. (2016). The synthesis and characterization of Mg-Zn-Ca alloy by powder metallurgy process. In *International Conference on Advanced Materials Science and Technology (ICAMST 2015)* (pp. 020032-1–6) Semarang, Indonesia: Semarang State University

Cai, S., Lei, T., Li, N., & Feng, F. (2012). Effects of Zn on microstructure, mechanical properties and corrosion behavior of Mg-Zn alloys. *Materials Science and Engineering C*, 32(8), 2570–2577.

Carter, D. R., & Hayes W.C. (1977) The compressive behavior of bone as a two-phase porous structure. *Clinical Orthopaedics and Related Research,* 59A*,* 954–962.

Dargusch, M.S., Balasubramani, N., Yang, N., Johnston, S., Ali, Y., Wang, G., Venezuela, J., Carluccio, J., Lau C., Allavena, R., Liang, D., Mardon, K., & Ye, Q. (2022). In vivo performance of a rare earth free Mg–Zn–Ca alloy manufactured using twin roll casting for potential applications in the cranial and maxillofacial fixation devices, *Bioactive Materials*, 12, 85-96.

Ding, Y., Wen, C., Hodgson, P., & Li, Y. (2014). Effects of alloying elements on the corrosion behavior and biocompatibility of biodegradable magnesium alloys: a review. *Journal of Material Chemistry B*, 2, 1912-1933.

Doležal, P., Zapletal, J., Fintová, S., Trojanová, Z., Greger, M., Roupcová, P., & Podrábskỳ, T. (2016). Influence of processing techniques on microstructure and mechanical properties of a biodegradable Mg-3Zn-2Ca alloy. *Materials*, 9(11), 880.

Erryani, A., Lestari, F. P., Annur, D., Kartika, I., & Sriyono, B. (2015). Structural properties of Mg-Ca-Zn alloy with addition of CaCO3 as foaming agent prepared by powder metallurgy method. In *International Conference Material and Metallurgical Technology* (pp. 423–434). Surabaya, Indonesia: Department of Materials and Metallurgical Engineering, ITS.

Fedunik-Hofman, L., Bayon, A., & Donne, S. W. Comparative Kinetic Analysis of $CaCO_3$/CaO Reaction System for Energy Storage and Carbon Capture. *Applied Sciences*, 9(21), 4601.

Ginebra, M. P., & Montufar, E. B. (2019) Cements as bone repair materials. In Pawelec, K.M., & Planell, J.A. (Eds.) In *Woodhead Publishing Series in Biomaterials: Bone Repair Biomaterials* (pp. 233-271). 2nd Ed. Woodhead Publishing.

Gonzalez, S., Pellicer, E., Surinach, S., Baro, M. D., & Sort, J. (2013). Biodegradable and Mechanical Integrity of Magnesium and Magnesium Alloys Suitable for Implants. In *Biodegradation Engineering and Technology*. (pp. 316-317). IntechOpen.

Harandi, S. E., Mirshahi, M., Koleini, S., Idris, M. H., Jafari, H., & Kadir, M. R. A. (2013). Effect of calcium content on the microstructure, hardness and in-vitro corrosion behavior of biodegradable mg-ca binary alloy. *Materials Research*, 16(1), 11–18.

Hofstetter, J., Becker, M., Martinelli, E., Weinberg, A.M., Mingler, B., Kilian, H., Pogatscher, S., Uggowitzer, P. J., & J. F. Löffler, J. F. (2014). High-Strength Low-Alloy (HSLA) Mg–Zn–Ca Alloys with Excellent Biodegradation Performance. *JOM,* 66, 566–572.

Hussein, R. O., & Northwood, D. O. (2014). Improving

the performance of magnesium alloys for automotive applications. *WIT Transactions on the Built Environment*, 137, 531–544.

Kennedy, A. (2012). *Porous Metals and Metals Foams Made from Powder* (p. 38). University of Nottingham: IntechOpen.

Lestari, P. L., Marta, S., Eryanni, A., Mulyati, I., & Kartika, I. (2020). In Vitro Corrosion of Quaternery Magnesium Alloy Foam by Addition of Zinc. *Journal of Electronics, Electromedical, and Medical Informatics,* 2(3), 86-92.

Lietaert, K., Weber, L., Van Humbeeck, J., Mortensen, A., Luyten, J., & Schrooten, J. (2013). Open cellular magnesium alloys for biodegradable orthopaedic implants. *Journal of Magnesium and Alloys*, 1(4), 303–311.

Lu, G. Q., Hao, H., Wang, F. Y., & Zhang, X. G. (2013). Preparation of closed-cell Mg foams using SiO_2-coated $CaCO_3$ as blowing agent in atmosphere. *Transactions of Nonferrous Metals Society of China (English Edition)*, 23(6), 1832–1837.

Lu, Y. U. (2014). Microstructure and Degradation Behaviour of Mg-Zn(-Ca) Alloys. *PhD Thesis*. University of Birmingham.

Peron, M., Torgersen, J., & Berto, F. (2017). Mg and its alloys for biomedical applications: Exploring corrosion and its interplay with mechanical failure. *Metals*, 7(7), 252.

Rad, H. R. B., Idris, M. H., Kadir, M. R. A., & Farahany, S. (2012). Microstructure analysis and corrosion behavior of biodegradable Mg–Ca implant alloys. *Materials & Design*, 33, 88-97.

Sahinoja, M. T. (2013). Study of Magnesium Metal and Its Alloys As a Biodegradable Material for Medical and Electrical. *Master's Thesis*. Tampere University of Technology.

Salleh, E. M., Ramakrishnan, S., & Hussain, Z. (2016). Synthesis of Biodegradable Mg-Zn Alloy by Mechanical Alloying : Effect of Milling Time. *Procedia Chemistry*, 19, 525–530.

Salvetr, P., Novák, P., & Vojtěch, D. (2016). Porous magnesium alloys prepared by powder metallurgy. *Materiali in Tehnologije*, 50(6), 917–922.

Schaublin, R. E., Becker, M., Cihova, M., Gerstl, S. S. A., Deiana, D., Hebert, C., Pogatscher, S., Uggowitzer, P. J., & Loffler, J. F. (2022). Precipitation in lean Mg-Zn-Ca alloys. *Acta Materialia,* 239, 118223.

Seyedraoufi, Z. S., & Mirdamadi, S. (2013). Synthesis, microstructure and mechanical properties of porous Mg-Zn scaffolds. *Journal of the Mechanical Behavior of Biomedical Materials*, 21, 1–8.

Tu, T., Chen, X. H., Chen, J., Zhao, C. Y., & Pan, F. S. (2019). A High-Ductility Mg–Zn–Ca Magnesium Alloy. *Acta Metallurgica Sinica*, 32, 23-30.

Yang, D., Chen, W., Lu, J., Hu, Z., Feng, Y., Chen, J., Jiang, J., Ma, A., Wang, L., Wang, H. (2017). Fabrication of Cellular Mg Alloy By Gas Release Reaction Via Powder Metallurgi Approach. *Metal Powder Report*, 72 (2), 124-127.

Yusop, A. H., Bakir, A. A., Shaharom, N. A., Abdul Kadir, M. R., & Hermawan, H. (2012). Porous biodegradable metals for hard tissue scaffolds: A review. *International Journal of Biomaterials*, 2012, 641430.

Zeng, R.C., Qi, W.C., Cui, H.Z., Zhang, F., Li, S.Q., & Han, E.H. (2015). In vitro corrosion of as-extruded Mg–Ca alloys—The influence of Ca concentration. *Corrosion Science*, 96, 23-31.

doi: 10.14710/teknik.v44i2.49587